# Solving the Puzzle of Cyg X-3: Gamma-Ray Clues into Jet Dynamics

**A. Dmytriiev**[1], A.A. Zdziarski[2], D. Malyshev[3], V. Bosch-Ramon[4,5], M. Chernyakova[6]

[1] NWU, South Africa, [2] CAMK, Warsaw, Poland, [3] Institut für Astronomie und Astrophysik Tübingen, Germany, [4] Universitat de Barcelona, Spain, [5] Instituto Argentino de Radioastronomía, Argentina, [6] DIAS, Dublin, Ireland

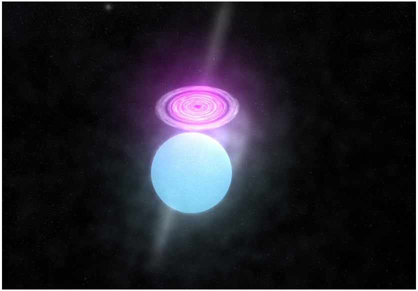

VGGRS VII – Barcelona, Spain (08 May 2025)

# Outline

# Outline

# Cyg X-3: a puzzling microquasar

- High-mass XRB
- Nature of the compact object is unknown (**NS/BH ?**)
  - BH hypothesis is favored, but NS is not ruled out
- Donor: Wolf-Rayet (WR) star
  - The only system in the Galaxy consisting of WR star and a compact object
- Masses of components uncertain. $M_* \sim 12 M_\odot$, $M_c \sim 7 M_\odot$ ?
- Luminous in radio and X-ray. Strong X-ray polarization $\sim 25$ % (Veledina+23)
- **Shows prominent $\gamma$-ray emission**

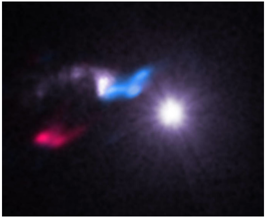

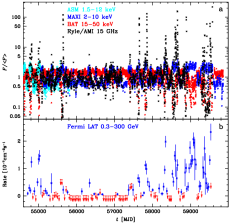


Figure: Top: composite X-ray and radio image of Cyg-X3 (credit: NASA/CXC/SAO/M.McCollough et al, Radio: ASIAA/SAO/SMA). Bottom: multi-band long-term LCs of Cyg X-3 (credit: A.A. Zdziarski)

# X-ray polarization in Cyg X-3

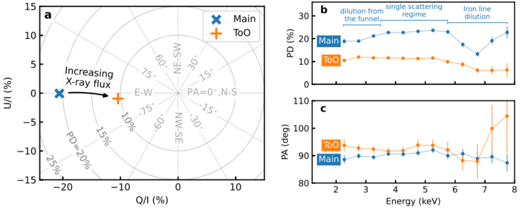


Figure: Orbital-phase averaged polarization properties of Cyg X-3 as measured by IXPE (credit: Veledina+23)

**IXPE revealed strong (∼ 25 %) X-ray polarization** (Veledina+23):

⇒ The central source is obscured, and we only see X-rays reflected from the inner surface of a narrow *accretion funnel*

The accretion is **super-Eddington** → Cyg X-3 is a superluminous X-ray source. The funnel is aligned with the radio jet.

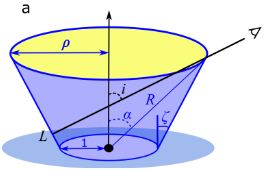


Figure: A schematic representation of the accretion funnel (credit: Veledina+23)

# $\gamma$-ray emission from Cyg X-3

Recent enhanced $\gamma$-ray activity of the source. Data can provide new clues about the system

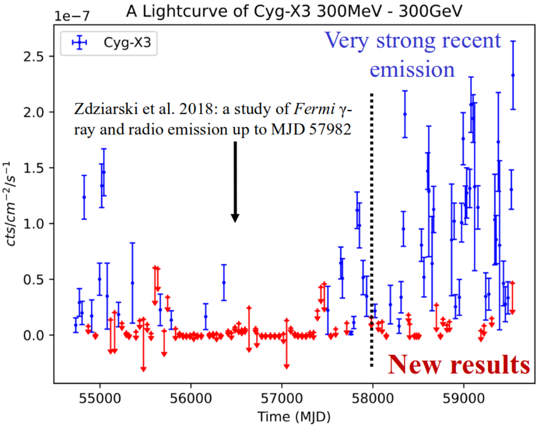


Figure: $\gamma$-ray light curve of Cyg X-3 (credit: A.A. Zdziarski)

# What $\gamma$-ray data tell us?

- $\gamma$-rays are strongly **orbitaly modulated** (Fermi LAT Collaboration et al. (2009))
- Modulation: anisotropic Compton scattering of blackbody photons from the donor (Dubus et al. (2010))
- Maximum of the emission expected at superior conjunction (SC) (compact object behind the donor star)
- The data shows an offset of the peak wrt SC → signature of **jet misalignment**
- X-rays undergo **wind absorption** → their *minimum* is at SC

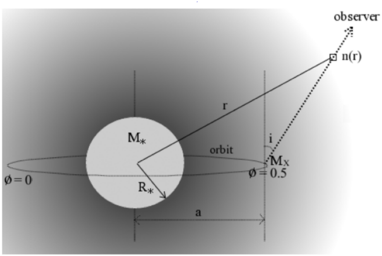


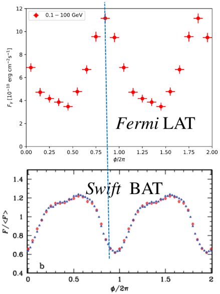


Left: a scheme visualizing the orbital modulation of X-ray and $\gamma$-ray emissions. Right: folded $\gamma$ (top) and X-ray (bottom) orbital modulation LCs (credit: A.A. Zdziarski)

# Motivation of our study: better data and modeling

- Previous studies (Dubus et al. (2010), Zdziarski et al. (2018)) use $\gamma$-ray data with too limited statistics
- We use recent data with **drastically better quality** (photon statistics)
- New **MWL** constraints ! (sub-mm)
- **Improved modeling:**
  - We take into account **Klein-Nishina** effects for the anisotropic IC
  - **Cooled** electron population
  - Self-consistent computation of the **cooling break**

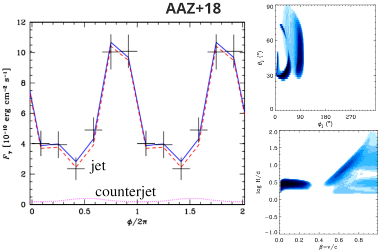


Figure: Modeling old $\gamma$-ray Cyg X-3 data (LC modulation) (credit: Zdziarski et al. (2018))

$\Rightarrow$ Much better constraints on the parameters of the system

# Outline

# Analysis of *Fermi*-LAT $\gamma$-ray data of Cyg X-3

- We analyze *Fermi*-LAT data of Cyg X-3 for MJD 57982 – 59533 (Aug 2017 – Nov 2021)
- *Spectral analysis*: **0.05 – 500 GeV**
- *Timing analysis*: 0.1 - 100 GeV
- We analyze only $\gamma$-ray bright states (defined in same way as "flaring state" in Z18)
- $F$(0.1 - 100 GeV) $> 5 \times 10^{-10}$ erg cm$^{-2}$ s$^{-1}$ AND TS $> 16$

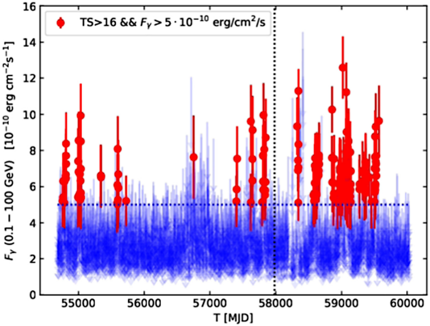


Figure: The LAT high-energy gamma-ray light curve of Cyg X-3 from the beginning of the Fermi observations until MJD 60200. The red and blue symbols represent the detections within a day and upper limits, respectively.

# Search for periodicity in 0.1 – 100 GeV $\gamma$-ray signal

- We use the *quadratic ephemeris* given by model 4 of Antokhin & Cherepashchuk (2019) and **search for periodicity** in the *Fermi*-LAT light curve taking into account their rate of increasing period
- Periodicity search: Lomb-Scargle periodogram gives $\boldsymbol{P_0 = 0.199684622(15)}$ **d**. Full agreement with X-rays
- We calculate the folded and averaged light curve in 10 phase bins

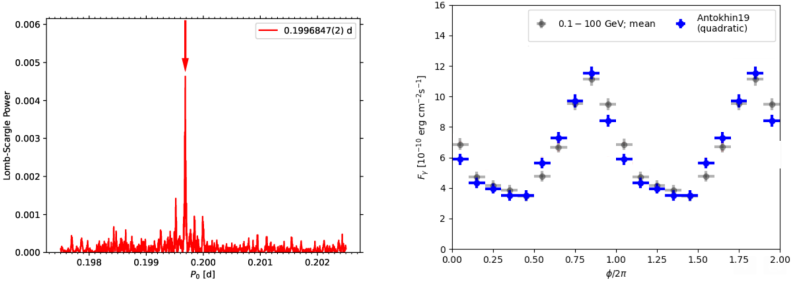


Figure: Left: The Lomb–Scargle periodogram in the gamma-ray bright state in the 0.1 – 100 GeV range, calculated accounting for the increase in secular orbital period and taking into account the measurement uncertainties. Right: folded phase LC of Cyg X-3 in $\gamma$-ray band based on new data

# Outline

# Physical model for $\gamma$-ray emission

- **Inverse Compton on stellar photons**:

  Relativistic $e^-$ in the jet Compton upscatter blackbody photons from the donor star to GeV energies

  (full KN angle-dependent cross-section!)

- **Magnetic field**

  Contribution from the **synchrotron self-Compton (SSC)**

- Total $\gamma$-ray emission:
  **IC on stellar photons + SSC**

- Emitting region: cylinder with height $Z \approx (1/3)H$, radius $R = \alpha_{\mathrm{oa,j}} H$

- Jet opening angle $\alpha_{\mathrm{oa,j}}$: **5°**

  (Miller-Jones, Fender & Nakar (2006))

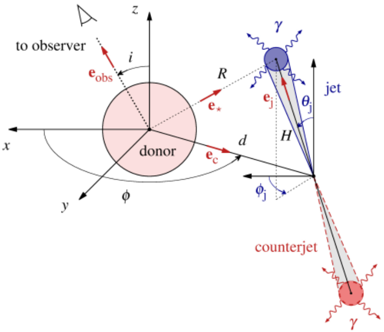


**SSC process**

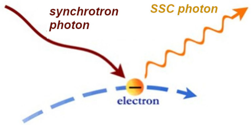


Figure: Top: Geometry of anisotropic Compton scattering in Cyg X-3 (Credit: A.A. Zdziarski). Bottom: scheme of SSC process

# Electron spectrum

- **Power law** with a low- and high-energy cutoffs at $\gamma_1$ and $\gamma_2$

  $$\boxed{N_e(\gamma) = K\gamma^{-p}}$$

  Stationary shock. Matter moves through the jet

- **Cooled population**:

  $$N_e(\gamma) \propto \dot{\gamma}_{\rm cool}(\gamma) \propto \boldsymbol{\gamma}^{-2} \qquad \text{for } \gamma_{\rm br} < \gamma < \gamma_1 \text{ (radiative cooling)}$$

  $$N_e(\gamma) \propto \boldsymbol{\gamma}^{-1} \qquad \text{for } \gamma_{\rm min} < \gamma < \gamma_{\rm br} \text{ (adiabatic losses)}$$

- **Lorentz factor of the break**:

  $$\boxed{t_{\rm cool}(\gamma) = t_{\rm ad}}$$

  $$\dot{\gamma}_{\rm cool}(\gamma) = \frac{4\sigma_{\rm T}}{3m_{\rm e}c}\gamma^2(U_B + U_{\rm rad})$$

  $(\gamma_{\rm br}\ x \ll 1)$

  $$U_B = B^2/(8\pi)$$

  $$U_{\rm rad} = U_{\rm rad,*} + U_{\rm rad,syn}$$

  $$U_{\rm rad,*} = (1/c)\ \sigma_{\rm B} T_*^4\ (R_*^2\ /< R^2 >)$$

  $$U_{\rm rad,syn} = \int_{\nu_{\rm min}}^{\nu_{\rm max}} U_{\rm rad,syn}(\nu)\ d\nu$$

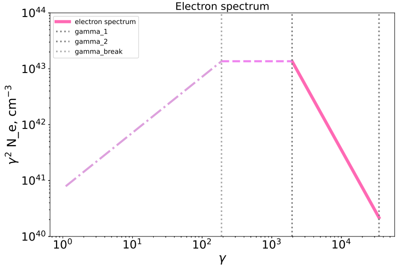


Figure: Example of the electron spectrum.

Previous constraint: $\boldsymbol{B < 100}$ **G** (Zdziarski et al. (2012))

(*only spectra, no LC, no fitting)

**Available constraints from data**:

- **Submillimeter array (SMA)**: $< F >$ (225 GHz) $\approx$ 300 mJy (McCollough 2023)
- **X-ray**: $F$(100 keV) $\approx$ 0.1 keV cm$^{-2}$ s$^{-1}$ (AAZ+12)
- **$\gamma$-ray**: LC minimum flux $F_{\mathrm{LC,min}} \approx 3.5 \times 10^{-10}$ erg cm$^{-2}$ s$^{-1}$
  $\Rightarrow$ **maximum SSC flux**

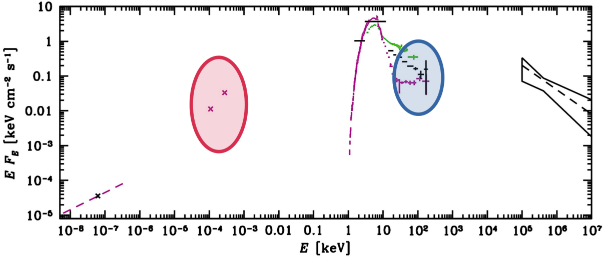


Figure: Available MWL measurements for Cyg X-3 during 2008 and 2009 $\gamma$-ray active periods (credit: AAZ+12)

# Outline

## Model 1

**Stable Jet**

# Model 1 (Origin of the orbital modulation of $\gamma$-rays)

- Jet is **misaligned** and has **constant orientation**
- Phase-dependent boosting of the stellar emission into the jet frame
- Phase-dependent (anisotropic) Compton scattering
- Boosting of IC emission into the observer frame (jet viewing angle)
- Strongest IC emission when electrons move towards the stellar photons

$\Rightarrow$ **Maximum of $\gamma$-rays when jet is behind the star**

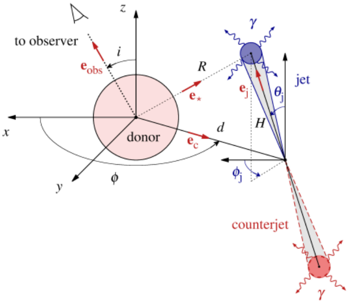


Figure: Geometry of anisotropic Compton scattering in Cyg X-3. Credit: A.A. Zdziarski

## Fitting the phase-averaged SED

We determine

- Total $e^-$ energy content $E_{\mathrm{e,tot}}$
- Spectral index $p = 4.8 \pm 0.1$
- Minimum Lorentz factor $\gamma_1 = 3400 \pm 400$
- Maximum Lorentz factor - **not required!** $\gamma_2 \to \infty$

$\chi^2_\nu = 7.5/7$

We assume/fix

- Temperature of the star $T_* = 10^5$ K
- Orbital separation $a = 2.66 \times 10^{11}$ cm
- Distance to Cyg X-3 $D_{\mathrm{sys}} = \mathbf{9}$ kpc (NEW!) (Reid & Miller-Jones (2023))

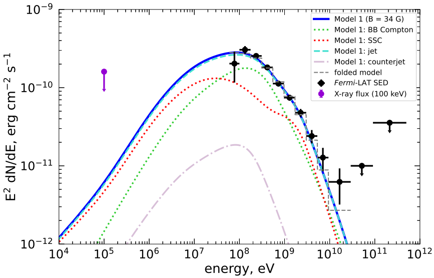


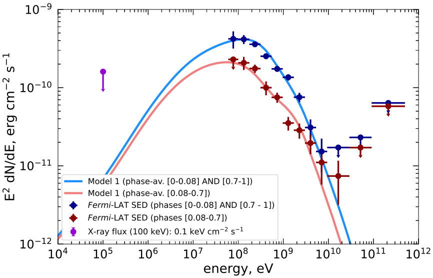

## Fitting the phase modulation LC

We determine

- Distance to em. region along the jet $H \approx (2.3 \pm 0.6) \cdot a \sim 10^6 R_g$
- **Jet inclination angle $\theta_{\rm j} = (35 \pm 8)^\circ$**
- Jet azimuthal angle $\phi_{\rm j} = (188 \pm 3)^\circ$
- Inclination of the system $i = (33 \pm 7)^\circ$
- Jet velocity $\beta_{\rm j} = 0.7 \pm 0.2$

$\chi^2_\nu = 7.3/5$

Jet viewing angle: $\boldsymbol{i_{\rm j} = 5^{+12}_{-2}}\ ^\circ$
*compatible with other constraints*

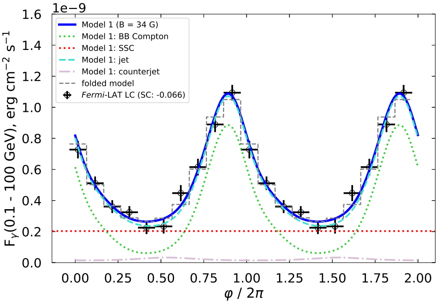


**Maximum magnetic field**: $B_{\rm max} = 34$ **G**

# Caveats for Model 1

We find evidence of jet misalignment wrt orbital axis. In this situation, the jet should precess due to the effects of **general relativity (GR)**

Precession: **de Sitter** (presence of central mass) and **Lense-Thirring** (rotation of central mass) effect

**De Sitter effect dominates** in our case. Period of precession for a binary system (Barker & O'Connel 75; Apostolatos+94):

$$P_{\rm prec} = \frac{c^2 (M_* + M_{\rm c})^{4/3} P^{5/3}}{(2\pi G)^{2/3} (2 + (3M_*)/(2M_{\rm c})) M_* M_{\rm c}} \quad (1)$$

For Cyg X-3 with $P = 0.2$ d, we get $P_{\rm prec} \approx 50$ yr

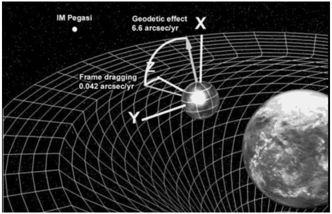

# Caveats for Model 1: search for the jet precession in the data

1. Over $P_{\rm prec} \approx 50$ yr, $\phi_{\rm j}$ will change by 360°

   Evolving jet orientation → peak of the modulation moves around.

   **We see NO variations in the modulation over 5000 d of *Fermi*-LAT monitoring.**

2. Jet precession → jet position angle evolution

   (angle difference between the projection of the jet and the orbital axis in the plane of the sky)

   **We see NO changes of this angle in radio data spanning 30 yr.**

---

⇒ **Jet not aligned with the spin axis of the compact object?** *Not easy to explain...*

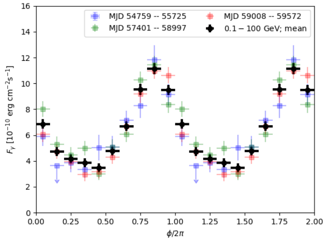


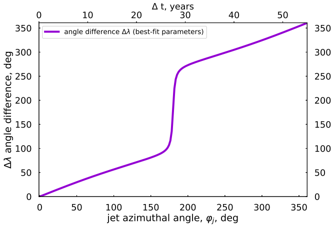


Figure: Top: comparison of $\gamma$-ray modulation over different time intervals (credit: D. Malyshev). Bottom: predicted projection angle evolution over 50 years due to jet precession (A. Dmytriiev).

# Model 2

## Wind-induced Bent and Precessing Jet

Intense **stellar wind** of WR star: **outward bending** of the jet (Yoon & Heinz 2015; Bosch-Ramon & Barkov 2016)

Orbital rotation: **Coriolis force** induces **lateral jet bending**.

→ **Jet aligned on average**

→ **Rapid jet precession at the orbital period** (0.2 d)

This can also explain X-ray polarization modulation at the orbital period

---

We model the jet bending as:

$$\varphi_{\rm j} = \varphi - \Delta$$

$\varphi$: orbital phase

$\Delta$: Coriolis jet bending angle (fit parameter)

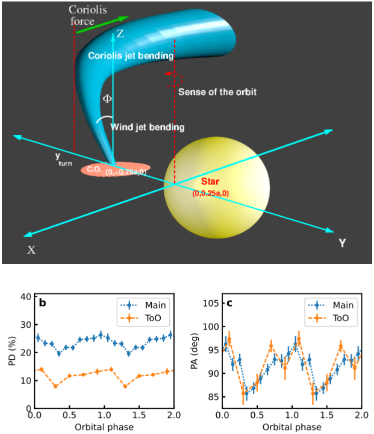


Figure: Top: Illustration of a simulated scenario of jet bending due to wind thrust and Coriolis force in a binary system. Credit: Barkov & Bosch-Ramon (2022). Bottom: X-ray polarization modulation measurements (Veledina+23).

# Modulation in sub-mm band vs in $\gamma$-rays

**Sub-millimeter Array (SMA)**

Preliminary SMA results shown by Michael McCollough (CXC/SAO/CfA) at The 10th Microquasar Workshop **(May 2023)**

**Modulation pattern in sub-mm band (225 GHz) is SAME as in $\gamma$-rays !**

---

**$\Rightarrow$ Only possible within pure SSC scenario (varying Doppler factor) !**

Figure: SMA instrument, Mauna Kea, Hawaii (credit: Afshin Darian, SMA)

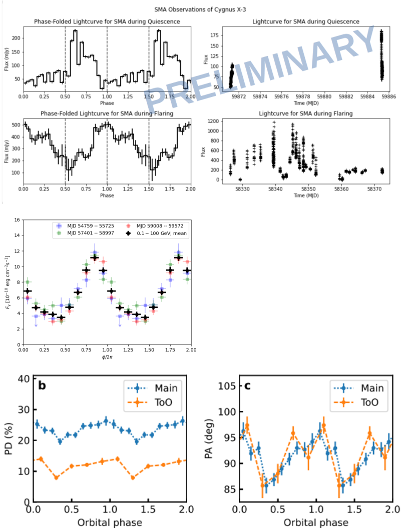


Figure: Top: Preliminary results of SMA flux modulation (sub-mm). Credit: M. McCollough. Middle: $\gamma$-ray modulation profile. Bottom: X-ray polarization modulation measurements (Veledina+23).

# Models of B(z)

We calculate the magnetic field as a function of the height $B(z)$ using analytical model by Zdziarski et al. (2022)

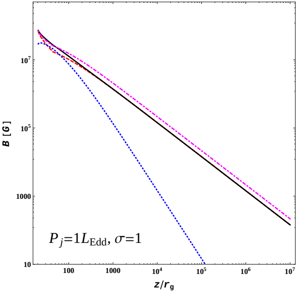


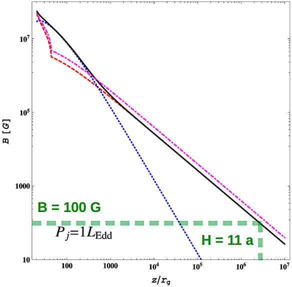


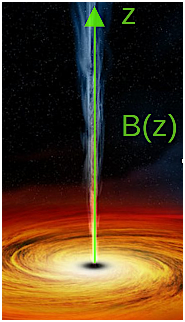


**Maximum** $B$ **solution**: $B = 100$ G, $h/a = 11$

# Model 2: synchrotron / sub-mm model predictions and LC fit

$h/a \gg 1$ needed for **high synchrotron power** (low Compton dominance) and to match $\boldsymbol{B}_{\mathbf{max}}$

$$L_{\rm SSC}/L_{\rm syn} \propto (h/a)^{-1}$$

We reproduce the phase-averaged SMA flux:

$< F(\nu = 225\ \mathrm{GHz}) > \approx$ 300 mJy

$$\boxed{\boldsymbol{B = 100\ \mathrm{G}}} \quad \text{with } h/a = 11$$

Synchrotron SED

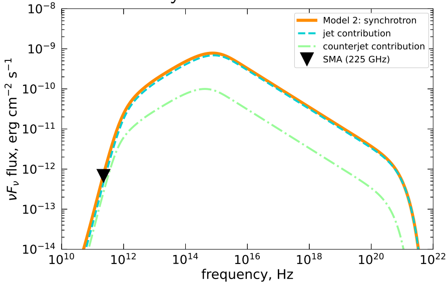


**sub-mm (225 GHZ)**

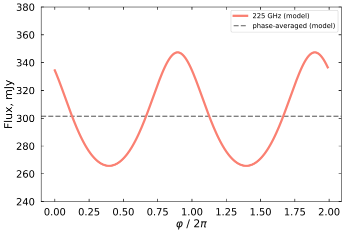


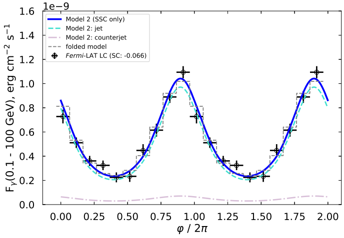


**γ-rays (0.1 – 100 GeV)**

## Pure SSC

**We determine**

- Spectral index $p \approx 4 \pm 0.1$
- Minimum Lorentz factor $\gamma_{\min} = 1100 \pm 200$
- **Jet inclination angle $\boldsymbol{\theta_j = (41 \pm 2)^\circ}$**
- Coriolis bending angle $\Delta = (142 \pm 4)^\circ$
- Jet velocity $\beta_j = 0.46 \pm 0.02$

  $\rightarrow$ slow jet

**We fix**

- Inclination of the system $i = 30^\circ$
- Distance to emitting region along the jet $\boldsymbol{h = 11 \cdot a}$

  $\rightarrow$ $H/a \gg 1$

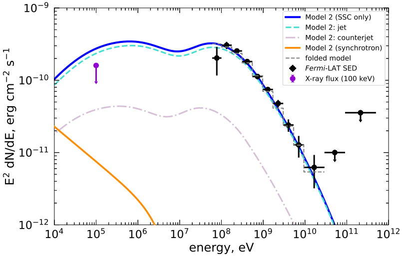


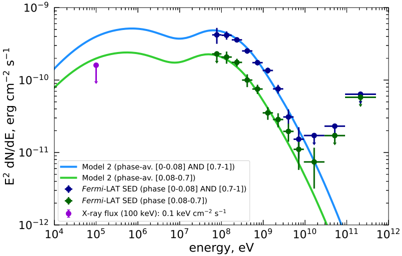


SED: $\chi^2_\nu = 8.1/7$; LC: $\chi^2_\nu = 10.3/7$

## Predictions for the wind-induced jet bending angel

Angle of the **jet outward bending** of the jet (Bosch-Ramon & Barkov 2016)

$$\Phi \approx \frac{\alpha_j \dot{M}_w v_w (\Gamma_j - 1)\, c}{4\pi \beta_j \Gamma_j P_j} \qquad (2)$$

We assume:

- $\dot{M}_w = 10^{-5}\, M_\odot/\mathrm{yr}$ (Antokhin 2022)
- $v_w = 1.5 \times 10^8$ cm/s (van Kerkwijk et al. 1996)
- $\Gamma_j = 2$ (in the jet launching region)

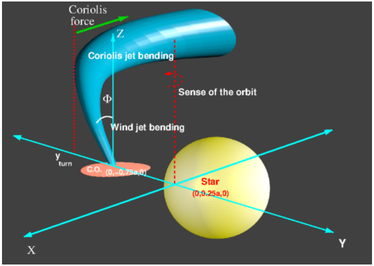


Figure: Illustration of a simulated scenario of jet bending due to wind thrust and Coriolis force in a binary system. Credit: Barkov & Bosch-Ramon (2022).

We find $\boldsymbol{\Phi \approx 1^\circ}$ $\rightarrow$ **incompatible** with $\boldsymbol{\theta_j \approx 41^\circ}$ from the $\gamma$-ray data fit

*Steve Prabu (COSPAR 2024): $\Phi \approx 2.5^\circ$ in Cyg X-1 based on radio data

# Outline

# Summary

- We propose two models to explain the origin of $\gamma$-rays at its modulation in the X-ray binary Cyg X-3
- **1. Stable Jet model**:
  - Anisotropic Compton (+SSC) $\gamma$-ray emission origin
  - Jet has to be **inclined** wrt to the orbital axis
  - **GR-induced precession (~50 yr) not observed in data!**
- **2. Wind-induced jet precession model**:
  - **Pure synchrotron self-Compton (SSC)** $\gamma$-ray origin
  - Rapid precession at the orbital period (0.2 d)
  - **Predicted jet bending angle is significantly lower than the one fromt the $\gamma$-ray data fit: $1^\circ$ vs $41^\circ$**
- Significantly improved constraints on the **magnetic field** in the $\gamma$-ray production region: $\boldsymbol{B \approx 100}$ **G**
- Substantially tighter constraints on the parameters of the system

---

$\rightarrow$ **ApJ (2024) 972, 1, id.85, 12**

DOI:10.3847/1538-4357/ad6440

amdmame@gmail.com

# Thank you for your attention!

# Back-up slides

# Modulation in sub-mm band vs in $\gamma$-rays

$$\boxed{F_{\rm syn}(\varphi) \text{ and } F_{\rm SSC}(\varphi) \propto \delta(\varphi)^2}$$

$$\delta(\varphi) = \frac{1}{\Gamma[1 - \beta_j \cos i_{\rm j}(\varphi)]}$$

$$\cos i_{\rm j} = \cos i \cos\theta_{\rm j} - \sin i \sin\theta_{\rm j} \cos(\varphi - \Delta)$$

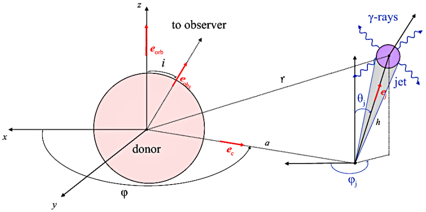


**Superior conjunction:**

– stellar Compton is in *maximum*

– synchrotron and SSC are in *minimum*

⇒ If $\gamma$-rays are produced via IC on stellar photons, then **sub-mm** and **$\gamma$-ray** modulations should be in **anti-phase**

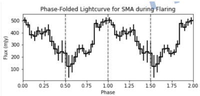


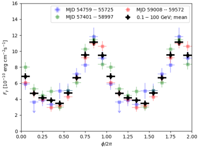


However, we observe them **in phase** !

---

**Dominant $\gamma$-ray production mechanism: SSC ?** → new unexpected result

# Derived quantities of interest

- Jet power, energy in $e^{-}$ (total kinetic energy + bulk motion): $P_{\rm e} \approx 1.2 \times 10^{38}$ erg s$^{-1}$
- Jet power, energy in (cold) ions (only bulk motion): $P_{\rm i} \approx 5.1 \times 10^{38}$ erg s$^{-1}$
- Jet power, magnetic energy: $P_B \approx 3.8 \times 10^{36}$ erg s$^{-1}$
- Jet power, total radiative output: $P_{\rm rad} \approx 6.3 \times 10^{38}$ erg s$^{-1}$
- Magnetization parameter: $\sigma \approx 0.001$
- Equipartition parameter: $\beta = u_{\rm e}/u_B \approx 31$

# Constraints on the parameters of the donor star

Contribution from the star to the target photon field **is subdominant**

For stationary jet model, we assumed: $R_* = 10^{11}$ cm and $T_* = 10^5$ K.

We derive a constraint on $R_* T_*^2$ by degrading the fit by $\Delta\chi^2 = 2.7$

$\Rightarrow$ $\boxed{R_* T_*^2 \leq 1.7 \times 10^{21} \text{ cm K}^2}$

$\chi^2$ decreases first! The most optimal fit with $R_* T_*^2 = 1.6 \times 10^{21}$ cm K$^2$